Vietnam Journal of Mechanics, VAST, Vol. 41, No. 1 (2019), pp. 51 – 62
DOI: https://doi.org/10.15625/0866-7136/12710

A THEORETICAL STUDY ON PROPAGATION OF GUIDED WAVES IN A FLUID LAYER OVERLYING A SOLID HALF-SPACE

Phuong-Thuy Nguyen[1], **Haidang Phan**[2,3,*]
[1]*Institute of Physics, VAST, Hanoi, Vietnam*
[2]*Graduate University of Science and Technology, VAST, Hanoi, Vietnam*
[3]*Institute of Mechanics, VAST, Hanoi, Vietnam*
[*]E-mail: haidangphan.vn@gmail.com

Received: 02 July 2018 / Published online: 29 October 2018

Abstract. Ultrasonic guided waves propagating in a non-viscous fluid layer of uniform thickness bonded to an elastic solid half-space is theoretically investigated in this article. Based on the boundary conditions set for the joined configuration, a characteristic dispersion equation is found and new expressions for free guided waves are introduced. Closed-form solutions of guided waves generated by a time-harmonic load are derived by the use of elastodynamics reciprocity theorems. Through calculation examples, it is shown that the obtained computation of the lowest wave mode approaches the result of the Rayleigh wave in the solid half-space as the layer thickness approaches zero. The aim of the present work is to improve the understanding of wave motions in layered half-spaces for potential applications in the area of bone quantitative ultrasound.

Keywords: layered half-space; guided waves; reciprocity theorem; quantitative ultrasound.

1. INTRODUCTION

Quantitative ultrasound (QUS) has shown a great potential in the assessment of bone characteristics in the recent research. Compared to X-ray method, QUS is more sensitive in the determinants of bone strength, non-ionizing and able to give some information about the elastic properties and defects of bones [1–3]. Various studies have been carried out to understand ultrasound interaction with the bone structure. Lowet and Van der Perre [4] studied the simulation of ultrasound wave propagation and the method to measure velocity in long bones. Numerical simulations of wave propagation and experiment measurement were used to gain insights into the expected behaviour of guided waves in bone [3]. Simulation results have made significant steps to improve our understanding of ultrasound interaction with bone [5]. Our knowledge of wave interaction with bone is, however, still far from complete because of the lack of analytic solutions.

Bones are normally composed of layers of different materials including cortical bone, cancellous bone and marrow. Propagation of guided waves in bone is largely influenced by the presence of overlying soft-tissue layer which is usually mimicked by a fluid layer of finite thickness. When the soft-tissue is relatively thin compared with the cortical bone, a fluid-solid layered half-space model can be used to study wave propagation in bone structures. In the current investigation, the soft tissue layer is considered as a non-viscous fluid while the cortical bone is assumed to be an isotropic solid half-space. This work aims to expand our understanding of guided wave propagation in a fluid-solid layered half-space to explore the potential of using ultrasound-based methods for long-bone characterization.

Wave motion in layered structures is indisputably one of the most fundamental problems of elastodynamics that has been widely considered for applications in geophysics, acoustics, and medicines. Theory of free ultrasonic waves propagating in layered structures can be found, for example, in the textbooks [6–11]. This classical topic is also addressed in a large number of research articles available in the literature. Approximate formula for guided wave velocity in an elastic half-space coated by a thin elastic layer with a smooth contact was considered in [12]. In a similar manner, approximate secular equations of the waves in an orthotropic half-space coated by a thin orthotropic layer with sliding contact were also derived and reported in [13] by the same authors. Achenbach and Keshava [14] analyzed dispersion curves for free waves in a layered half-space while Tiersten [15] investigated the influence of thin film on the propagation of guided waves in the film-halfspace structure with comparison to experiment data. Matrix method is used to investigate the dispersion of Rayleigh waves in orthotropic layered half-space [16]. Dispersion equations for a fluid-solid bilayered plate were derived and a discussion on the shapes of the wave modes was addressed in [17].

Wave motion generated by a loading is conventionally solved by using integral transform techniques [7]. The integral transform approach, however, becomes more difficult for anisotropic solids, and impossible for inhomogeneous solids, for example, solids whose elastic moduli depend on the depth coordinate, as in geophysical applications and functionally graded materials. In order to avoid these difficulties, another method has been proposed in recent years, based on the elastodynamic reciprocity theorem, strictly to determine the guided waves. Compared to the integral transform, the reciprocity approach is simpler [18–21] and more general that is able to use for anisotropic and inhomogeneous materials [22, 23].

Generally, reciprocity theorem is a relation between displacements, tractions and body forces for two different loading states of the same body. One of the states is referred as the actual state, guided waves radiated from a time-harmonic load and the other is called the virtual state, an appropriately chosen free wave traveling in the structure. Statements of elastodynamic reciprocity theorems have already presented, and curious readers can refer to, e.g., [24–26]. Reciprocity relations have been successfully used in direct applications to calculate wave motions generated by a time-harmonic load, see [18, 19, 22, 23, 27, 28]. The material to be studied may be inhomogeneous, anisotropic or viscoelastic. Balogun and Achenbach [22] examined surface waves generated by a line load on a half-space with depth-dependent properties. The applications of reciprocity

to surface waves on an inhomogeneous transversely isotropic half-space was discussed in [23]. Recently, Phan et al. [29] considered the computation of guided waves in structure of a solid layer joined to a solid half-space. The reciprocity approach was also applied to study scattering of surface waves by cavities on the surface of a half-space [30–33] and scattering of Lamb waves by a partial spherical corrosion pit in a plate [34].

In this article, we first find the characteristic dispersion equation and propose new explicit expressions for free guided waves. The expressions are essential to obtain closed-form solutions of wave fields generated by a time-harmonic load in the fluid-solid layered half-space by reciprocity consideration. The next step is choosing an appropriate virtual state which is a single guided wave mode propagating in the joined structure. The two loading states are substituted into a reciprocity relation for a two-material body. The relation is largely simplified due to the characteristics of guided waves in the fluid layer overlying the solid half-space. After some manipulation, exact solutions of the guided waves due to the time-harmonic load are derived. The examples of calculation show that the obtained result of the lowest wave mode approaches the computation of the Rayleigh wave in the solid half-space as the layer thickness approaches zero.

2. FREE GUIDED WAVES IN FLUID LAYER BONDED TO SOLID HALF-SPACE

Consider a fluid layer Ω of uniform thickness h and a solid half-space $\widehat{\Omega}$ which are bonded together along the plane $z = 0$. The layered half-space relative to the Cartesian coordinate system (x, z) is shown in Fig. 1. Free guided waves propagating in the layered half-space are discussed in this section. For a homogeneous isotropic elastic solid, the governing equations are the displacement equations of motion [7]

$$\widehat{\mu} u_{i,jj} + \left(\widehat{\lambda} + \widehat{\mu}\right) u_{j,ji} = \widehat{\rho} \ddot{u}_i \,, \tag{1}$$

where $\widehat{\lambda}, \widehat{\mu}$ are the Lame constants and $\widehat{\rho}$ is the mass density. For a non-viscous fluid, which does not sustain shear stresses, the equations of wave motion given in Eq. (1) can be used by assuming $\widehat{\mu} = 0$.

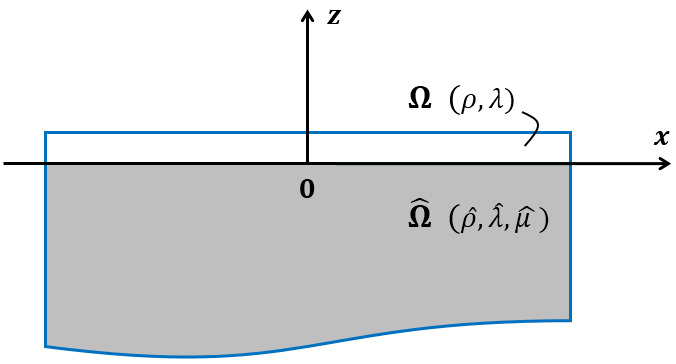

Fig. 1. Coordinate system for fluid layer joined to solid half-space

The trial solutions in the layered half-space can be expressed as a combination of partial waves based on the partial wave theory discussed in detail, for example, in [8]. In this case, there are two partial waves in the fluid layer and another two in the solid half-space. Besides the amplitudes, guided waves in this joined structure are defined by an angular frequency ω and a wavenumber k, where $k = \omega/c$, c being the phase velocity, as well as material properties λ, ρ of Ω and $\widehat{\lambda}, \widehat{\mu}, \widehat{\rho}$ of $\widehat{\Omega}$. For the fluid layer, displacement components may be written as

$$u_x = \left(A_1 e^{ik\alpha z} + A_2 e^{-ik\alpha z}\right) e^{ik(x-ct)}, \tag{2}$$

$$u_z = \alpha \left(A_1 e^{ik\alpha z} - A_2 e^{-ik\alpha z}\right) e^{ik(x-ct)}, \tag{3}$$

and for the half-space, they are of the form

$$\widehat{u}_x = \left(\widehat{A}_1 e^{k\widehat{\alpha}_1 z} + \widehat{A}_2 e^{k\widehat{\alpha}_2 z}\right) e^{ik(x-ct)}, \tag{4}$$

$$\widehat{u}_z = -i \left(\frac{1}{\widehat{\alpha}_1} \widehat{A}_1 e^{k\widehat{\alpha}_1 z} + \widehat{\alpha}_2 \widehat{A}_2 e^{k\widehat{\alpha}_2 z}\right) e^{ik(x-ct)}, \tag{5}$$

where A_j and $\widehat{A}_j$ $(j = 1, 2)$ are constants to be determined. In Eqs. (2)–(5),

$$\alpha = \sqrt{-1 + c^2/c_L^2}\,, \tag{6}$$

$$\widehat{\alpha}_1 = \sqrt{1 - c^2/\widehat{c}_T^2}\,, \quad \widehat{\alpha}_2 = \sqrt{1 - c^2/\widehat{c}_L^2}\,, \tag{7}$$

where $c_L = \sqrt{\lambda/\rho}$ is longitudinal wave velocity of Ω while $\widehat{c}_T = \sqrt{\widehat{\mu}/\widehat{\rho}}$ and $\widehat{c}_L = \sqrt{(\widehat{\lambda} + 2\widehat{\mu})/\widehat{\rho}}$ are the transverse and longitudinal wave velocities, respectively, of $\widehat{\Omega}$. In Eqs. (6)–(7), $\alpha, \widehat{\alpha}_1, \widehat{\alpha}_2$ are dimensionless quantities and they are generally complex. It is important to note that guided waves in the fluid-solid layered half-space may not have a real solution for phase velocity. Therefore, they may not exist for some material combination. A detailed study of the conditions of the material properties for the existence of guided waves is, however, beyond the scope of the current work.

From Eqs. (2)–(5), stress components τ_{xx}, τ_{zz} of the layer Ω and $\widehat{\tau}_{xx}, \widehat{\tau}_{xz}, \widehat{\tau}_{zz}$ of the half-space $\widehat{\Omega}$ can be easily calculated by the use of Hooke's law. For guided waves in the layered half-space, there are one free boundary condition at the free surface $(z = h)$ and three conditions at the interface $(z = 0)$

$$\tau_{zz} = 0 \qquad \text{at } z = h, \tag{8}$$

$$u_z = \widehat{u}_z\,, \quad \widehat{\tau}_{xz} = 0, \quad \tau_{zz} = \widehat{\tau}_{zz} \quad \text{at } z = 0. \tag{9}$$

Eqs. (8) and (9) result in

$$\begin{bmatrix} e^{ik\alpha h} & e^{-ik\alpha h} & 0 & 0 \\ \alpha & -\alpha & i/\widehat{\alpha}_1 & i\widehat{\alpha}_2 \\ 0 & 0 & \widehat{\alpha}_1 + 1/\widehat{\alpha}_1 & 2\widehat{\alpha}_2 \\ 1+\alpha^2 & 1+\alpha^2 & 2\dfrac{\widehat{\mu}}{\lambda} & \left(\widehat{\alpha}_1^2 + 1\right)\dfrac{\widehat{\mu}}{\lambda} \end{bmatrix} \begin{bmatrix} A_1 \\ A_2 \\ \widehat{A}_1 \\ \widehat{A}_2 \end{bmatrix} = \begin{bmatrix} 0 \\ 0 \\ 0 \\ 0 \end{bmatrix}. \tag{10}$$

In order to have nontrivial solutions, the determinant of the four-by-four matrix in Eq. (10) must be zero. It leads to which is referred to as the characteristic dispersion equation

$$\left(\frac{1}{\alpha}+\alpha\right)\left(1-\widehat{\alpha}_1^2\right)\widehat{\alpha}_2\tan k\alpha h+\left(\left(\widehat{\alpha}_1^2+1\right)^2-4\widehat{\alpha}_1\widehat{\alpha}_2\right)\frac{\widehat{\mu}}{\lambda}=0. \tag{11}$$

As the thickness of the layer approaches zero in the limit, i.e. $\tan k\alpha h = 0$, Eq. (11) becomes the famous equation of Rayleigh surface waves in a half-space. Unlike Rayleigh waves, guided waves in the layered half-space are dispersive because there is a frequency term via k appearing in Eq. (10). It also means that there is an infinite number of wave modes propagating in the structure of a layer joined to a half-space.

Table 1. Material properties of water and aluminum

Material	ρ (kg/cm^3)	λ (GPa)	μ (GPa)
Water	1000	2.25	0
Aluminum	2700	55.25	25.94

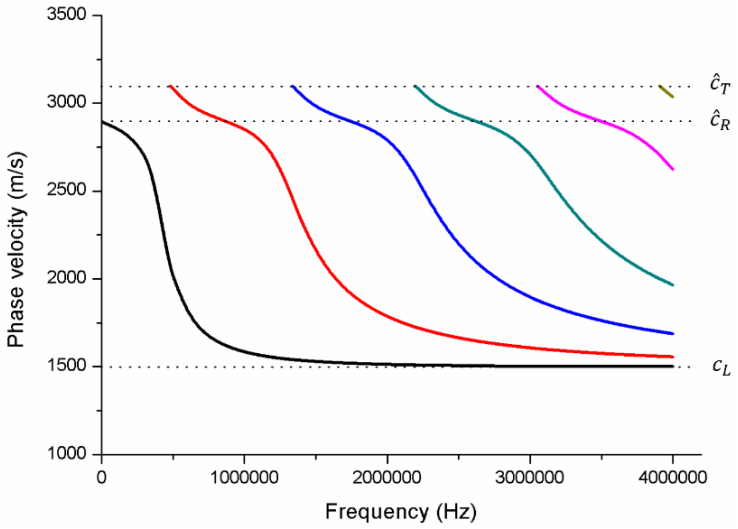

Fig. 2. Dispersion curves for a water layer of thickness and an aluminum half-space

As an example of calculation, the dispersion curves of a water layer and an aluminum half-space with the material properties tabulated in Tab. 1 are shown in Fig. 2. It can be seen that the phase velocity values are confined over a certain range. The upper bound of the phase velocity value is the shear wave velocity in the aluminum half-space while its lower limit is the longitudinal wave velocity in the water. The wave velocity approaches the Rayleigh surface wave in aluminum at the low frequency limit where the layer thickness is much smaller than the wavelength. When the phase velocity is larger

than the shear wave velocity of the aluminum half-space, wave energy will leak into the half-space. The guided wave mode with complex phase velocity attenuates and is not considered here as we are only interested initially in non-leaky wave modes.

Since the determinant of the matrix in Eq. (10) is zero, it has actually three independent equations with four unknowns. The process of solving Eq. (10) is straightforward but quite tedious. Therefore, we propose expressions for free guided waves in the layered half-space without a detailed proof. The displacements and stress components of the layer are

$$u_x = AU_x(z)e^{ik(x-ct)}, \tag{12}$$
$$u_z = AU_z(z)e^{ik(x-ct)}, \tag{13}$$
$$\tau_{xx} = ik\lambda AT_{xx}(z)e^{ik(x-ct)}, \tag{14}$$

where

$$U_x(z) = d_1e^{ik\alpha z} + d_2e^{-ik\alpha z}, \tag{15}$$
$$U_z(z) = \alpha\left(d_1e^{ik\alpha z} - d_2e^{-ik\alpha z}\right), \tag{16}$$
$$T_{xx}(z) = \left(1+\alpha^2\right)\left(d_1e^{ik\alpha z} + d_2e^{-ik\alpha z}\right). \tag{17}$$

For the half-space

$$\widehat{u}_x = A\widehat{U}_x(z)e^{ik(x-ct)}, \tag{18}$$
$$\widehat{u}_z = -iA\widehat{U}_z(z)e^{ik(x-ct)}, \tag{19}$$
$$\widehat{\tau}_{xx} = ik\widehat{\mu}A\widehat{T}_{xx}(z)e^{ik(x-ct)}, \tag{20}$$
$$\widehat{\tau}_{xz} = k\widehat{\mu}A\widehat{T}_{xz}(z)e^{ik(x-ct)}, \tag{21}$$

where

$$\widehat{U}_x(z) = \widehat{d}_1e^{k\widehat{\alpha}_1z} + \widehat{d}_2e^{k\widehat{\alpha}_2z}, \tag{22}$$
$$\widehat{U}_z(z) = \frac{1}{\widehat{\alpha}_1}\widehat{d}_1e^{k\widehat{\alpha}_1z} + \widehat{\alpha}_2\widehat{d}_2e^{k\widehat{\alpha}_2z}, \tag{23}$$
$$\widehat{T}_{xx}(z) = 2\widehat{d}_1e^{k\widehat{\alpha}_1z} + \left(2\widehat{\alpha}_2^2 - \widehat{\alpha}_1^2 + 1\right)\widehat{d}_2e^{k\widehat{\alpha}_2z}, \tag{24}$$
$$\widehat{T}_{xz}(z) = \left(\widehat{\alpha}_1 + \frac{1}{\widehat{\alpha}_1}\right)\widehat{d}_1e^{k\widehat{\alpha}_1z} + 2\widehat{\alpha}_2\widehat{d}_2e^{k\widehat{\alpha}_2z}. \tag{25}$$

In Eqs. (15)–(17) and Eqs. (22)–(25), $d_1, d_2, \widehat{d}_1, \widehat{d}_2$ are dimensionless quantities defined as

$$d_1 = \left(1-\widehat{\alpha}_1^2\right)\widehat{\alpha}_2\,, \tag{26}$$
$$d_2 = \beta^2\left(\widehat{\alpha}_1^2-1\right)\widehat{\alpha}_2\,, \tag{27}$$
$$\widehat{d}_1 = 2i\alpha\left(1+\beta^2\right)\widehat{\alpha}_1\widehat{\alpha}_2\,, \tag{28}$$
$$\widehat{d}_2 = -i\alpha\left(1+\beta^2\right)\left(1+\widehat{\alpha}_1^2\right), \tag{29}$$

where $\beta = e^{ik\alpha h}$. In Eqs. (12)–(14) and Eqs. (18)–(21), there is only one unknown constant A. The explicit expressions of guided waves are essential to direct application of

reciprocity to obtain closed-form solutions of wave fields generated by a time-harmonic load in the next section.

3. COMPUTATION OF GUIDED WAVES DUE TO TIME-HARMONIC LOADING

In this section, a reciprocity theorem is applied to obtain the amplitudes of guided waves due to a time-harmonic line load. We first consider a vertical load applied at (x_0, z_0) where x_0, z_0 are the x-coordinate and the z-coordinate, respectively, of the point of application. The load is of the form

$$f_z^A = P\delta(z - z_0)\delta(x - x_0)e^{-ikct}. \tag{30}$$

The load will generate guided waves along the layered half-space in both the positive x-direction and the negative x-direction with unknown relative scattered amplitudes A_m^{P+} and A_m^{P-}, respectively. Here, $m = 0, 1, \ldots, \infty$ indicate wave mode. This is the actual state A whose amplitudes are to be determined by the use of reciprocity consideration. The expansions for the far-field displacements of state A in the positive direction may be written as

$$u_x = \sum_{m=0}^{\infty} u_x^m = \sum_{m=0}^{\infty} A_m^{P+} U_x^m(z) e^{ik_m(x - c_m t)}, \tag{31}$$

$$u_z = \sum_{m=0}^{\infty} u_z^m = \sum_{m=0}^{\infty} A_m^{P+} U_z^m(z) e^{ik_m(x - c_m t)}, \tag{32}$$

$$\widehat{u}_x = \sum_{m=0}^{\infty} \widehat{u}_x^m = \sum_{m=0}^{\infty} A_m^{P+} \widehat{U}_x^m(z) e^{ik_m(x - c_m t)}, \tag{33}$$

$$\widehat{u}_z = \sum_{m=0}^{\infty} \widehat{u}_z^m = -i \sum_{m=0}^{\infty} A_m^{P+} \widehat{U}_z^m(z) e^{ik_m(x - c_m t)}. \tag{34}$$

Reciprocity theorem offers a relation between displacements, tractions and body forces of two different loading states. Based on the reciprocity relation of the two states, the scattered amplitudes of guided waves of the actual state are derived. The ideal was introduced in [24] for a half-space and a plate body and recently developed for layered structures [28, 29]. For a two-material body, the reciprocity follows from Eq. (38) of [28]

$$\begin{aligned} \int_{\Omega} \left(f_j^A u_j^B - f_j^B u_j^A \right) \mathrm{d}\Omega + \int_{\widehat{\Omega}} \left(\widehat{f}_j^A \widehat{u}_j^B - \widehat{f}_j^B \widehat{u}_j^A \right) \mathrm{d}\widehat{\Omega} = \\ \int_{S} \left(\tau_{ij}^B u_j^A - \tau_{ij}^A u_j^B \right) n_i \mathrm{d}S + \int_{\widehat{S}} \left(\widehat{\tau}_{ij}^B \widehat{u}_j^A - \widehat{\tau}_{ij}^A \widehat{u}_j^B \right) \widehat{n}_i \mathrm{d}\widehat{S}, \end{aligned} \tag{35}$$

where S and $\widehat{S}$ defines contours around Ω and $\widehat{\Omega}$ without the interface, respectively, while n_i and $\widehat{n}_i$ are normal vectors along S and $\widehat{S}$, respectively. Superscripts A and B denote two elastodynamic states. State A, the actual state, is the field generated by f_z^A while state B, the virtual state, is the field of a free guided wave in the layered half-space.

The first step is choosing a virtual state, i.e., state B based on the explicit expressions of free guided waves given in Eqs. (12)–(14) and Eqs. (18)–(21). State B is set to include

only a single wave mode represented by amplitude B_n. If state B is chosen in the negative x-direction, it is of the form

$$u_x^n = -B_n U_x^n(z) e^{-ik_n(x+c_n t)}, \tag{36}$$

$$u_z^n = B_n U_z^n(z) e^{-ik_n(x+c_n t)}, \tag{37}$$

$$\widehat{u}_x^n = -B_n \widehat{U}_x^n(z) e^{-ik_n(x+c_n t)}, \tag{38}$$

$$\widehat{u}_z^n = -iB_n \widehat{U}_z^n(z) e^{-ik_n(x+c_n t)}. \tag{39}$$

We then replace the expressions of states A and B into the reciprocity relation given in Eq. (35). The left-hand side of Eq. (35) can be simplified since the loading is applied only at (x_0, z_0). If state $A$and state B propagate in the same direction, the right-hand side of Eq. (35) vanishes. Thus, there is only contribution from the counter-propagating waves, see [24, 28] for detail. It can be easily seen that there is no contribution of the integration along to the top surface of the layered half-space because a free boundary condition is applied and along the line at $z \to \infty$ since the waves vanish. Moreover, using the orthogonality condition in Eq. (9.4.23) of [24], the right-hand side of Eq. (35) cancels out for $m \neq n$. Note that the time-harmonic loading can be anywhere in the joined structure. Without loss of generality, the load is applied in the half-space $\widehat{\Omega}$. After some manipulation, we finally obtain the amplitude of guided waves in the positive x-direction

$$A_n^{P+} = \frac{-iP\widehat{U}_z^n(z_0) e^{-ik_n x_0}}{2\left(\lambda I_n + \widehat{\mu}\widehat{I}_n\right)}, \tag{40}$$

where

$$I_n = ik_n \int_0^h \left[T_{xx}^n(z) U_x^n(z)\right] \mathrm{d}z, \tag{41}$$

$$\widehat{I}_n = ik_n \int_{-\infty}^0 \left[\widehat{T}_{xx}^n(z)\widehat{U}_x^n(z) + \widehat{T}_{xz}^n(z)\widehat{U}_z^n(z)\right] \mathrm{d}z. \tag{42}$$

The integrals in Eqs. (41) and (42) can be calculated as

$$I_n = \frac{1+\alpha^2}{2\alpha}\left[\left(e^{2ik\alpha h} - 1\right) d_1^2 - \left(e^{-2ik\alpha h} - 1\right) d_2^2 + 4ik\alpha h d_1 d_2\right], \tag{43}$$

$$\widehat{I}_n = i\left[\frac{3\widehat{\alpha}_1^2 + 1}{2\widehat{\alpha}_1^3}\widehat{d}_1^2 + \frac{2\widehat{\alpha}_1\widehat{\alpha}_2 - \widehat{\alpha}_1^2 + 3}{\widehat{\alpha}_1}\widehat{d}_1\widehat{d}_2 + \frac{4\widehat{\alpha}_2^2 - \widehat{\alpha}_1^2 + 1}{2\widehat{\alpha}_2}\widehat{d}_2^2\right]. \tag{44}$$

Note that $I_n, \widehat{I}_n$ are connected to the guided wave of mode n. Therefore, $k, \alpha, \widehat{\alpha}_1, \widehat{\alpha}_2, d_1, d_2, \widehat{d}_1, \widehat{d}_2$ are the quantities of mode n although we have ignored subscript n in the expressions of Eqs. (43) and (44). If a virtual wave of mode n in the positive x-direction is chosen, we find

$$A_n^{P-} = \frac{-iPU_z^n(z_0) e^{ik_n x_0}}{2\left(\lambda I_n + \widehat{\mu}\widehat{I}_n\right)}. \tag{45}$$

Similarly, for a horizontal load of the form

$$f_x^A = Q\delta(z - z_0)\delta(x - x_0)e^{-ikct}, \tag{46}$$

we find

$$A_n^{Q+} = \frac{-Q\widehat{U}_x^n(z_0)e^{-ik_n x_0}}{2\left(\lambda I_n + \widehat{\mu}\widehat{I}_n\right)}, \tag{47}$$

$$A_n^{Q-} = \frac{Q\widehat{U}_x^n(z_0)e^{ik_n x_0}}{2\left(\lambda I_n + \widehat{\mu}\widehat{I}_n\right)}. \tag{48}$$

4. RESULTS

This section presents calculation of phase velocity and displacement amplitudes of guided waves due to time-harmonic loading. Consider a water layer and an aluminum half-space whose material properties are given in Tab. 1. It is discussed in Section 2 that there is only the lowest wave mode propagating in the layered half-space as the thickness of the water layer is much smaller than the wavelength. As the layer thickness approaches zero in the limit, the phase velocity c approaches the velocity of Rayleigh surface wave $\widehat{c}_R$ in the half-space, see Fig. 2.

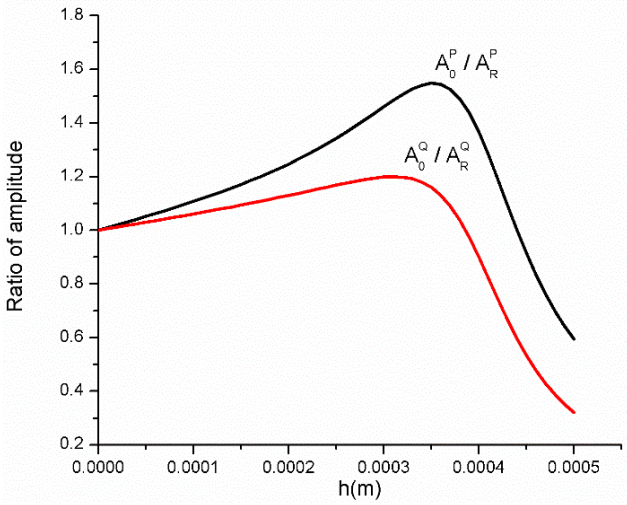

Fig. 3. Amplitude ratio of lowest mode to Rayleigh wave mode due to time-harmonic loading

We are now interested in showing that the displacement amplitudes of the lowest wave mode will approach the amplitudes of Rayleigh waves as the thickness of the layer h goes to zero in the limit for a fixed finite values of frequency f. The frequency is chosen as $f = 1$ MHz and the thickness of the layer varies from $h = 0$ to $h = 0.5$ mm. The magnitude of both vertical and horizontal loads is chosen as $P = Q = \widehat{\mu}/2$. The loads generate the lowest wave modes with scattered amplitudes A_0^P and A_0^Q, respectively. These amplitudes are compared with the ones of surface waves in an aluminum half-space, A_R^P and A_R^Q, obtained by Phan et al. [19]. The amplitude ratios of the lowest mode to the Rayleigh wave, A_0^P / A_R^P due to vertical load P and A_0^Q / A_R^Q due to horizontal load

Q, are displayed in Fig. 3. Clearly, $A_0^P / A_R^P \to 1$ and $A_0^Q / A_R^Q \to 1$ as the thickness of the layer approaches to zero. This shows the validation of the reciprocity approach discussed in the current study.

5. CONCLUSION

We have proposed a theoretical approach for ultrasonic guided waves propagating in a fluid layer overlying a solid half-space. Based on the boundary conditions, a characteristic dispersion equation has been found and explicit expressions for free guided waves in the structure have been obtained. One of the main contributions of the present work is the derivation of exact solutions of wave fields generated by a time-harmonic load in the fluid-solid layered half-space. It has been shown in calculation examples that as the layer thickness goes to zero, the computation of the lowest wave mode approaches the result of the Rayleigh surface wave.

The theoretical solutions obtained in the present research will be useful to build models for a cortical bone with overlying soft tissue as the cortical bone plate is relatively thick compared with the soft-tissue layer. The models allow us to discover the relation among transducer characteristics, frequencies, and geometry and material properties of bone tissues. They will definitely deliver a fast and computationally inexpensive calculation of generation, propagation, reflection, refraction, transmission and absorption as ultrasound interacts with bone tissue. The analytical simulation could also provide a better understanding of the experiment signals, improve the data interpretation and acquisition. The work will ultimately benefit physicians and scientists in developing ultrasonic methods for diagnosis and treatment of bone diseases and monitoring of bone healing after surgery.

ACKNOWLEDGMENTS

This research is funded by Vietnam National Foundation for Science and Technology Development (NAFOSTED) under grant number 107.02-2016.23; and Graduate University of Science and Technology under grant number GUST.STS.ĐT2017-CH01.

REFERENCES

[1] L. H. Le, Y. J. Gu, Y. Li, and C. Zhang. Probing long bones with ultrasonic body waves. *Applied Physics Letters*, **96**, (11), (2010). https://doi.org/10.1063/1.3300474.

[2] V. H. Nguyen, T. N. H. T. Tran, M. D. Sacchi, S. Naili, and L. H. Le. Computing dispersion curves of elastic/viscoelastic transversely-isotropic bone plates coupled with soft tissue and marrow using semi-analytical finite element (SAFE) method. *Computers in Biology and Medicine*, **87**, (2017), pp. 371–381. https://doi.org/10.1016/j.compbiomed.2017.06.001.

[3] P. H. F. Nicholson, P. Moilanen, T. Kärkkäinen, J. Timonen, and S. Cheng. Guided ultrasonic waves in long bones: modelling, experiment and in vivo application. *Physiological Measurement*, **23**, (4), (2002), pp. 755–768. https://doi.org/10.1088/0967-3334/23/4/313.

[4] G. Lowet and G. Van der Perre. Ultrasound velocity measurement in long bones: measurement method and simulation of ultrasound wave propagation. *Journal of Biomechanics*, **29**, (10), (1996), pp. 1255–1262. https://doi.org/10.1016/0021-9290(96)00054-1.

[5] J. J. Kaufman, G. Luo, and R. S. Siffert. Ultrasound simulation in bone. *IEEE Transactions on Ultrasonics, Ferroelectrics, and Frequency Control*, **55**, (6), (2008), pp. 1205–1218. https://doi.org/10.1109/tuffc.2008.784.
[6] A. H. Nayfeh. *Wave propagation in layered anisotropic media: With application to composites*. Elsevier, (1995).
[7] J. Achenbach. *Wave propagation in elastic solids*. North-Holland Publishing Company, (2012).
[8] J. L. Rose. *Ultrasonic guided waves in solid media*. Cambridge University Press, (2014).
[9] W. M. Ewing, W. S. Jardetzky, and F. Press. *Elastic waves in layered media*. McGraw-Hill, (1957).
[10] T. Kundu. *Ultrasonic nondestructive evaluation: engineering and biological material characterization*. CRC Press, (2003).
[11] N. T. K. Linh, P. C. Vinh, and L. T. Hue. An approximate formula for the H/V ratio of Rayleigh waves in compressible pre-stressed elastic half-spaces coated with a thin layer. *Vietnam Journal of Mechanics*, **40**, (1), (2018), pp. 63–78. https://doi.org/10.15625/0866-7136/10417.
[12] P. C. Vinh, V. T. N. Anh, and V. P. Thanh. Rayleigh waves in an isotropic elastic half-space coated by a thin isotropic elastic layer with smooth contact. *Wave Motion*, **51**, (3), (2014), pp. 496–504. https://doi.org/10.1016/j.wavemoti.2013.11.008.
[13] P. C. Vinh and V. T. N. Anh. Rayleigh waves in an orthotropic half-space coated by a thin orthotropic layer with sliding contact. *International Journal of Engineering Science*, **75**, (2014), pp. 154–164. https://doi.org/10.1016/j.ijengsci.2013.11.004.
[14] J. D. Achenbach and S. P. Keshava. Free waves in a plate supported by a semi-infinite continuum. *Journal of Applied Mechanics*, **34**, (2), (1967), pp. 397–404. https://doi.org/10.1115/1.3607696.
[15] H. F. Tiersten. Elastic surface waves guided by thin films. *Journal of Applied Physics*, **40**, (2), (1969), pp. 770–789. https://doi.org/10.1063/1.1657463.
[16] T. T. Tuan and T. N. Trung. The dispersion of Rayleigh waves in orthotropic layered half-space using matrix method. *Vietnam Journal of Mechanics*, **38**, (1), (2016), pp. 27–38. https://doi.org/10.15625/0866-7136/38/1/6191.
[17] C. L. Yapura and V. K. Kinra. Guided waves in a fluid-solid bilayer. *Wave Motion*, **21**, (1), (1995), pp. 35–46. https://doi.org/10.1016/0165-2125(94)00043-5.
[18] H. Phan, Y. Cho, and J. D. Achenbach. Verification of surface wave solutions obtained by the reciprocity theorem. *Ultrasonics*, **54**, (7), (2014), pp. 1891–1894. https://doi.org/10.1016/j.ultras.2014.05.003.
[19] H. Phan, Y. Cho, and J. D. Achenbach. Validity of the reciprocity approach for determination of surface wave motion. *Ultrasonics*, **53**, (3), (2013), pp. 665–671. https://doi.org/10.1016/j.ultras.2012.09.007.
[20] H. Phan, Y. Cho, and J. D. Achenbach. A theoretical study on scattering of surface waves by a cavity using the reciprocity theorem. In *Nondestructive Testing of Materials and Structures*, Springer Netherlands, (2013), pp. 739–744.
[21] H. Phan, Y. Cho, T. Ju, and J. D. Achenbach. Multiple scattering of surface waves by cavities in a half-space. In *AIP Conference Proceedings*, AIP, AIP, Vol. 1581, (2014), pp. 537–541. https://doi.org/10.1063/1.4864866.
[22] O. Balogun and J. D. Achenbach. Surface waves generated by a line load on a half-space with depth-dependent properties. *Wave Motion*, **50**, (7), (2013), pp. 1063–1072. https://doi.org/10.1016/j.wavemoti.2013.03.001.

[23] S. S. Kulkarni and J. D. Achenbach. Application of the reciprocity theorem to determine line-load-generated surface waves on an inhomogeneous transversely isotropic half-space. *Wave Motion*, **45**, (3), (2008), pp. 350–360. https://doi.org/10.1016/j.wavemoti.2007.07.001.
[24] J. D. Achenbach. *Reciprocity in elastodynamics*. Cambridge University Press, (2003).
[25] J. D. Achenbach, A. K. Gautesen, and H. McMaken. *Ray methods for waves in elastic solids: with applications to scattering by cracks*. Pitman Advanced Publishing Program, (1982).
[26] A. T. de Hoop. *Handbook of radiation and scattering of waves: Acoustic waves in fluids, elastic waves in solids, electromagnetic waves*. Academic Press, (1995).
[27] L. R. F. Rose, W. K. Chiu, N. Nadarajah, and B. S. Vien. Using reciprocity to derive the far field displacements due to buried sources and scatterers. *The Journal of the Acoustical Society of America*, **142**, (5), (2017), pp. 2979–2987. https://doi.org/10.1121/1.5009666.
[28] H. Phan, T. Q. Bui, H. T. L. Nguyen, and C. V. Pham. Computation of interface wave motions by reciprocity considerations. *Wave Motion*, **79**, (2018), pp. 10–22. https://doi.org/10.1016/j.wavemoti.2018.02.008.
[29] H. Phan, Y. Cho, Q. H. Le, P. C. Vinh, H. T. L. Nguyen, P. T. Nguyen, and T. Q. Bui. A closed-form solution to propagation of guided waves in a layered half-space under a time-harmonic load: An application of elastodynamic reciprocity. *Ultrasonics*, (2019). https://doi.org/10.1016/j.ultras.2019.03.015.
[30] H. Phan, Y. Cho, and J. D. Achenbach. Application of the reciprocity theorem to scattering of surface waves by a cavity. *International Journal of Solids and Structures*, **50**, (24), (2013), pp. 4080–4088. https://doi.org/10.1016/j.ijsolstr.2013.08.020.
[31] H. Phan, Y. Cho, and W. Li. A theoretical approach to multiple scattering of surface waves by shallow cavities in a half-space. *Ultrasonics*, **88**, (2018), pp. 16–25. https://doi.org/10.1016/j.ultras.2018.02.018.
[32] H. Phan, Y. Cho, T. Ju, J. D. Achenbach, S. Krishnaswamy, and B. Strom. A novel approach of using the elastodynamic reciprocity for guided wave problems. In *AIP Conference Proceedings*, AIP, AIP, Vol. 1511, (2013), pp. 107–112. https://doi.org/10.1063/1.4789037.
[33] W. Liu, Y. Cho, H. Phan, and J. D. Achenbach. Study on the scattering of 2-D Rayleigh waves by a cavity based on BEM simulation. *Journal of Mechanical Science and Technology*, **25**, (3), (2011), pp. 797–802. https://doi.org/10.1007/s12206-011-0133-5.
[34] S. Hao, B. W. Strom, G. Gordon, S. Krishnaswamy, and J. D. Achenbach. Scattering of the lowest Lamb wave modes by a corrosion pit. *Research in Nondestructive Evaluation*, **22**, (4), (2011), pp. 208–230. https://doi.org/10.1117/12.880534.